Development of Testbed AUV for Formation Control and Fundamental Experiment in Actual Sea Model Basin

by

OKAMOTO Akihiro[*], IMASATO Motonobu[*], HIRAO Shunka C.[*], SEKIGUCHI Hidenori[**]
SETA Takahiro[***], SASANO Masahiko[*], and FUJIWARA Toshifumi[*]

Abstract

The formation control of multiple autonomous underwater vehicles (AUVs) is becoming an increasingly vital factor in enhancing the efficiency of ocean resource exploration. However, deploying such a package of AUVs for operation at sea is difficult because of their large size. The aim of our study is to create a demonstration system for formation control algorithms using actual hardware. To implement a prototype system, we developed a testbed AUV usable in a test basin and performed a simple formation control test in the Actual Sea Model Basin constructed by the National Maritime Research Institute in Japan. Two AUVs, the simulated "virtual" leader and the developed "real" follower, communicate through an acoustic link and cruise to maintain a constant distance between them. Tests for more sophisticated formation control algorithms will be enabled using the system, consequently leading to implementation at sea.

This paper is a revised and republished version of the following paper:

Akihiro Okamoto, Motonobu Imasato, Shunka C. Hirao, Hidenori Sekiguchi, Takahiro Seta, Masahiko Sasano, and Toshifumi Fujiwara, "Development of Testbed AUV for Formation Control and its Fundamental Experiment in Actual Sea Model Basin," J. Robot. Mechatron., Vol.33, No.1, pp. 151-157, 2021.

---

* Offshore Advanced Technology Department

** Offshore Advanced Technology Department at the time of research, Present affiliation is Marine Environment & Engine System Department in NMRI

*** Offshore Advanced Technology Department at the time of research, Present affiliation is Toyota Research Institute Advanced Development, Inc.

Received January 26th, 2022.
Accepted March 14th, 2022.

Contents

1. Introduction

Autonomous underwater vehicles (AUVs) contribute significantly to underwater research, such as topographic surveys using sonars [1], visual mapping using cameras [2–5], and benthic sampling [6].

To improve the efficiency of planar mapping survey, the National Maritime Research Institute (NMRI) proposed a method involving the simultaneous deployment of multiple AUVs and an autonomous surface vehicle (ASV) [7]. This strategy is effective in terms of the total extent of the surveyed area. However, the broader the extent of the area, the more difficult it is to control and monitor the AUVs from the ASV. This is because the available zone of acoustic positioning and communication link from the ASV is limited, and each AUV cruises its assigned area independently. Hence, multiple AUVs must be controlled and maintained in formation during a survey mission.

To date, some formation control algorithms for AUVs have been proposed [8–15] and computationally simulated. However, challenges occur in placing such algorithms into practical use because they are just only simulated on computers. In addition, it is difficult to conduct tests in actual sea areas just for algorithm verification, because the operation of AUVs for actual observations requires a lot of manpower and a great deal of cost. Therefore, the hardware and environment for testing such algorithms are required before AUVs with such formation control systems are deployed at sea.

This paper outlines a demonstration scheme using a testbed AUV and a test basin for validating formation control algorithms. The newly developed AUV, which is equipped with an underwater communication modem required for formation control, and its fundamental test in a test basin are described in the following sections.

2. Testbed AUV for Formation Control

To implement the verification system of the AUV formation control in test basins, we developed a testbed AUV equipped with fundamental devices required for navigation and communication. As this AUV is for demonstration and the basin space is limited, the following requirements must be considered when designing its hardware and software:

- Sufficient compactness allowing handling by a few operators and maneuverability for turning in a small radius. In practice, multiple testbed AUVs operate simultaneously in a test basin.
- Communication network among AUVs. Each AUV shall obtain the status of the others and transmit its own information through acoustic links.

• Adaptive behavior correction based on received information. Each AUV shall be synchronized with the others to maintain the formation of AUVs.

By satisfying these conditions, any formation algorithms can be implemented and tested using AUVs in a test basin.

Figure 1 and Table 1 show the general arrangement and specifications of the developed AUV, namely, the NMRI small cruising AUV, "mini-AUV." It has a torpedo-shaped body, a thruster, and four independently movable fins, i.e., elevators and rudders. Its overall length is 1.8 m, which is reasonably small, and its weight is 38 kg. Hence, it can be operated by only two or three hands. Highly accurate navigation is enabled using an inertial navigation system with a fiber-optic gyroscope, aided by a Doppler velocity log (DVL). To construct an underwater communication network, an acoustic modem with an ultrashort baseline positioning system [16] is installed. In addition, buoyancy adjusting weights for submerging and surfacing, LED flashers, and satellite beacon enable the AUV to conduct trials in areas of water up to a depth of 120 m.

With regard to controlling the devices, a modified version of the software of AUV Hobalin [17], which was built using Robot Operating System (ROS) [18], was installed on an ARM-based embedded board. Fundamental functions such as following pre-planned waypoints in order, reporting their own state, and visiting a designated waypoint by orders via an acoustic communication link had already been implemented. Considering formation control, we assumed a leader-follower structure, where multiple follower AUVs followed a single leader AUV as a reference during cruising. A leader AUV transmits its state information such as its position and depth to the follower AUVs. To render AUVs cruise in formation, a function that generates waypoints dynamically based on received information was additionally implemented. Because the software system is composed of subdivided functions and nodes of ROS, each algorithm part can be easily replaced with a newly developed one.

AUV motion tests such as turning circle maneuvers, zig-zag tests, and planar motion mechanism (PMM) tests were conducted to obtain the kinematic performance of the AUV. For example, it was verified that the maximum speed exceeded 1.5 m/s and the minimum turning circle radius was 3.3 m, which is sufficiently small enough for tank tests. In addition, the equation of motion of the testbed AUV was obtained, which can be used to reconstruct the behavior during a mission sequence in the simulation (see Appendix).

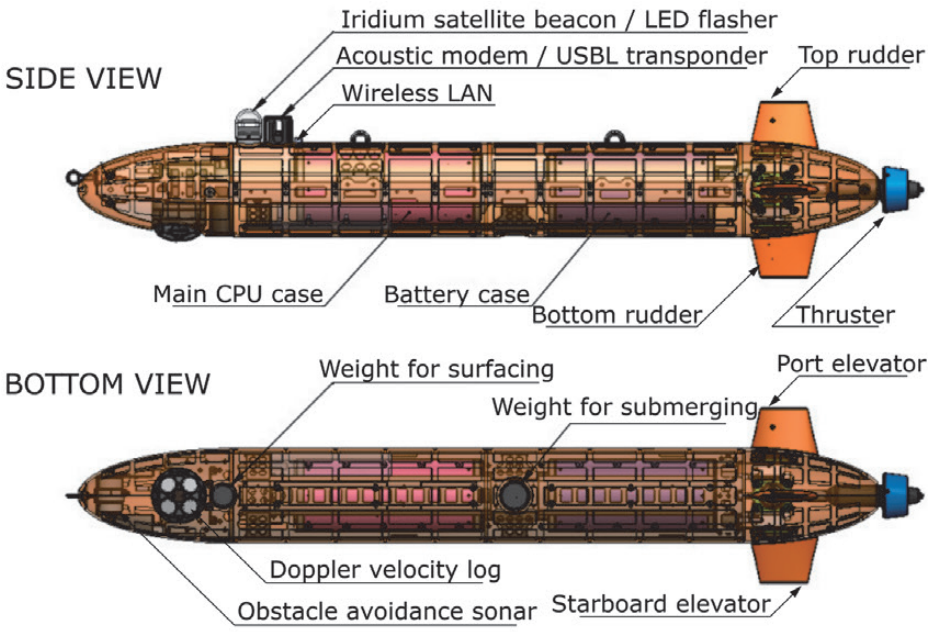

Fig. 1 Onboard equipment of testbed mini-AUV.

Table 1 Specifications of testbed mini-AUV.

General	
Weight in air	38 kg
Length	1.8 m
Diameter	0.2 m
Depth rating	120 m
Speed	1.5 m/s (max) 1.0 – 1.5 m/s (cruising)
Turning radius	3.3 m (min.)
Endurance	2 h (cruising)
Equipment	
Communication positioning	Blueprint SeaTrac X150
CPU board	Atmark Techno Armadillo-X1
OS	ROS Melodic Morenia on Debian stretch
Navigation	iXblue Phins C3
Bottom tracking	Nortek DVL 1000
Obstacle avoidance	Tritech Micron Sonar
Thruster	Tecnadyne Model260
Power source	IKS Japan Co.,Ltd. Li-ion 18650 × 72V, 10.4 Ah

3. Experiment in Test Basin

3.1. Actual Sea Model Basin

The Actual Sea Model Basin (shown in Fig. 2) was used to test the fundamental formation control functions of the testbed AUV. This basin is typically used to perform various ship motion tests using model ships as well as to reconstruct and analyze maritime accidents [19, 20]. This basin was selected for an experiment environment because of its dimension, i.e., 80.0 m (length) × 40.0 m (width) × 4.50 m (depth), which was sufficiently broad for an AUV to move around horizontally. This experiment was the first attempt to use an AUV in the Actual Sea Model Basin.

Fig. 2 Actual Sea Model Basin of the NMRI, measuring 80.0 m (length) × 40.0 m (width) × 4.50 m (depth).

3.2. Overview of Test Scenario

As the leader-follower structure was assumed in the formation control system, two AUVs at the least were required for each part. However, in the experiment, only one of the series of the testbed AUVs had been built at that time; hence, the leader part was simulated using the kinetic model obtained by the motion tests (Appendix). Meanwhile, the follower part was the physically existing AUV, which sought and chased such a "virtual" leader AUV.

Figure 3 shows a schematic of the experimental setup. The acoustic communication modem was submerged and fixed at the center of the basin and connected to a laptop computer, which simulated the virtual leader AUV. Information such as position, depth, and targeted waypoint ID were broadcasted and received by the follower AUV.

It is noteworthy that the position of the actual modem differed from the position of the imaginary modem of the leader AUV because the virtual leader AUV cruised around as simulated, whereas the modem was fixed.

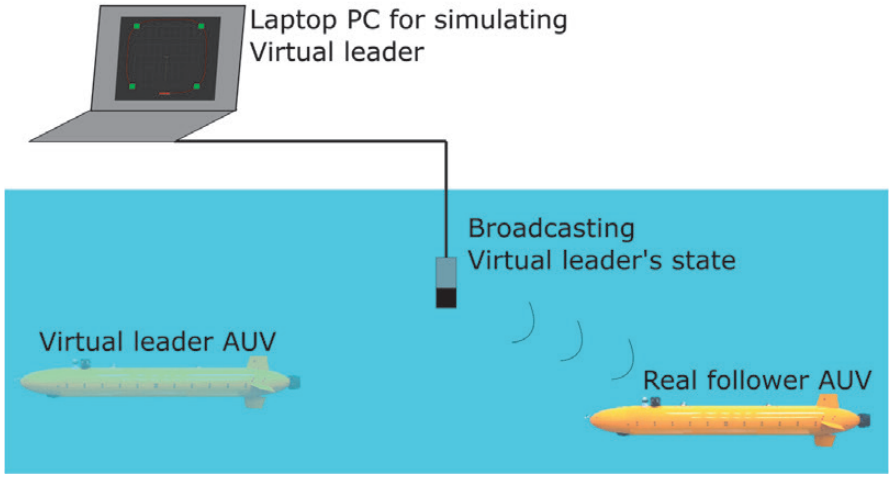

Fig. 3 Real follower AUV approaching simulated virtual leader AUV.

3.3. Virtual Leader AUV

As mentioned previously, the leader AUV did not have its own hardware except for the acoustic modem, which was installed 1.0 m deep in the basin. A planned course was composed of four waypoints in a square with a 10-m-long side, and the leader AUV cruised several laps in a clockwise direction at a 2.0 m depth. In addition, navigational information such as position (latitude and longitude) and depth was transmitted at intervals of 3 s. During the experiment, the state and trajectory of the leader AUV as well as the planned waypoints were visualized using Rviz, a three-dimensional visualization tool for ROS (Fig. 4).

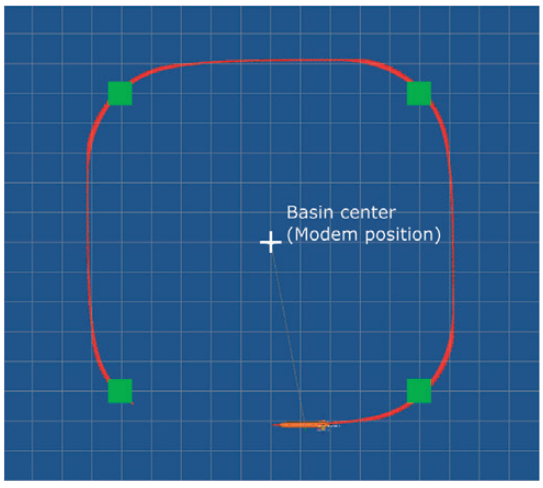

Fig. 4 Simulated motion and trajectory of virtual leader AUV displayed on Rviz (grid spacing = 1.0 m).

3.4. Real Follower AUV

The AUV described in Section 2 was assigned to the “real” follower AUV. It was submerged to start at the center of the basin and waited for broadcasted information through the acoustic communication link (Fig. 5). The moment any information from the leader AUV was received, the follower AUV dynamically generated a new waypoint toward the position of the leader AUV and started to track it. Each time the latest information was received, the target waypoint was updated and the behavior was immediately altered.

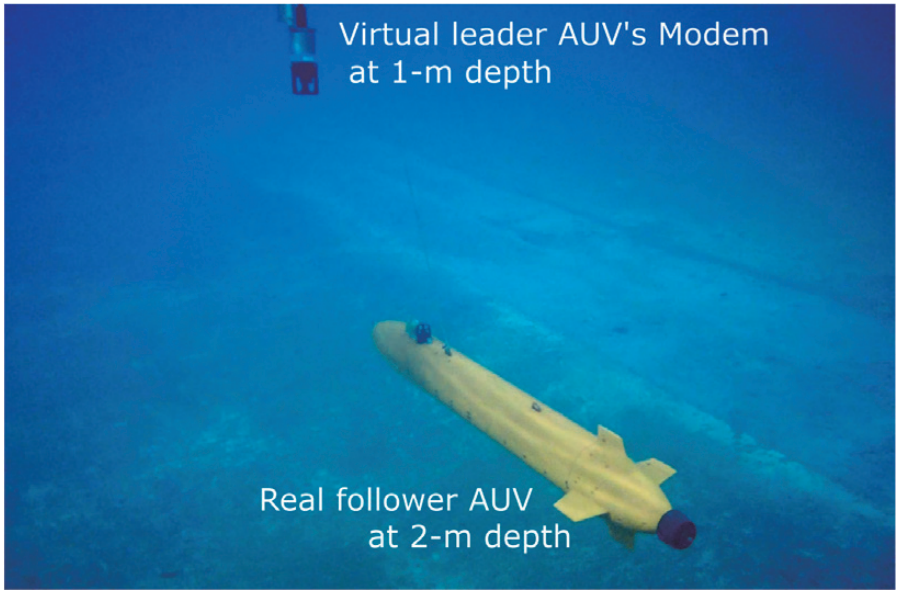

Fig. 5 Underwater image of fixed acoustic modem;
follower AUV about to chase virtual leader AUV from starting point.

3.5. Results

The results of one of the laps are shown in Fig. 6. The dashed red line and the solid black line represent the trajectories of the leader and follower, respectively. The marks on the trajectories as well as the red circle, blue square, and blue cross are the moments at which acoustic communication occurred. Each number beside those marks indicates the moment the leader transmitted its state and the follower received the corresponding state, respectively. Fig. 7(a) shows the distances between the AUVs during the lap. Each mark denotes the moment at which the aforementioned transmissions occurred. The mean distance was 6.94 m, and the standard deviation was 0.33 m. Figs. 7(b) and (c) illustrate the maneuver of the follower AUV. In Fig. 7(b), each time the target heading was updated based on a new waypoint of the received information, the follower AUV veered toward the direction of the waypoint. Fig. 7(c) shows the ordered values and output rudder angles. The orders to control the top and bottom rudders were calculated based on the deviation from the target heading and proportional gain. The actual output angle of the rudders was limited to ± 30◦, although the larger the deviation, the larger were the ordered values.

Although not all the messages were conveyed successfully, it was observed that the follower AUV successfully maneuvered itself and cruised before the leader AUV. The fact that the leader-follower structure control can be implemented in the test basin was verified by these results.

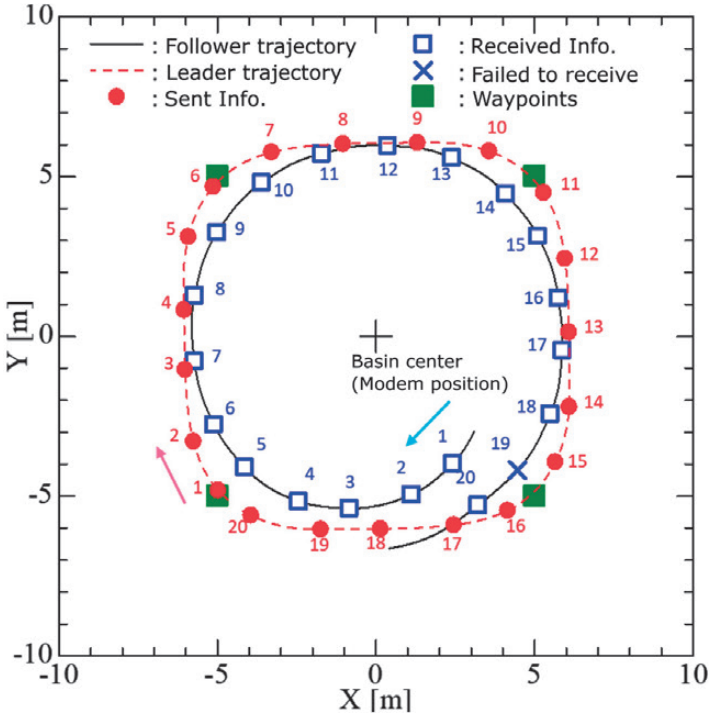

Fig. 6 Result of sending and receiving acoustic messages.

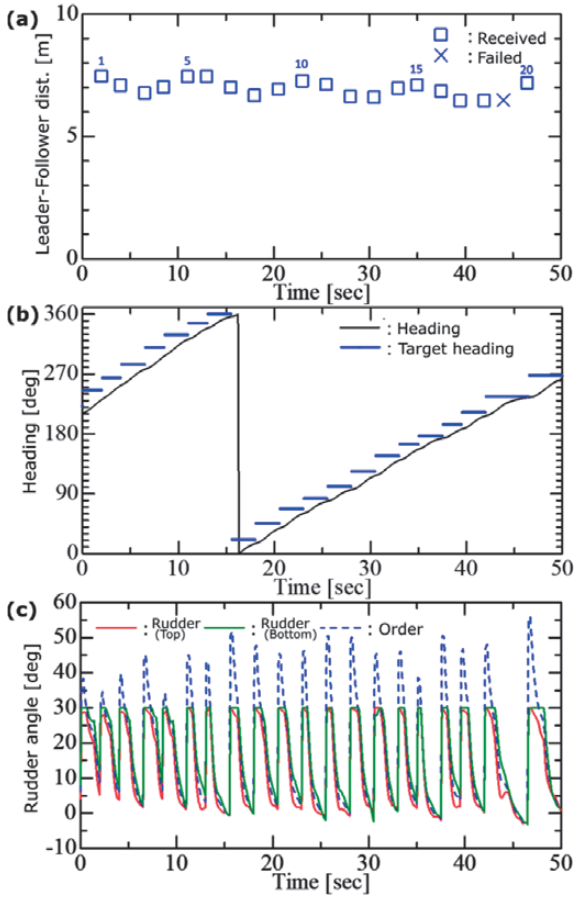

Fig. 7 Time-series data of experimental results. (a) Distances between leader and follower AUVs. (b) Fluctuation of headings of follower AUV. (c) Fluctuation of rudder angles of follower AUV.

4. Concluding Remarks

In this study, a testbed AUV was developed for formation control and a fundamental experiment in the Actual Sea Model Basin owned by the NMRI was performed. We obtained satisfactory results demonstrating that a real follower AUV tracked a virtual leader AUV whose motion was simulated on a laptop computer based on information through an acoustic link. This system made it possible to verify formation control algorithms using actual AUVs more easily and at a lower cost than in actual seas.

However, the experiment was performed under a desirable underwater communication quality. Acoustically severe environments can be presumed, such as longer distances among acoustic modems. Such conditions, which will degrade communication quality and cause intermittent information exchanges, should be considered in the future.

This study is the first step toward enhancing our development of a formation control system for multiple AUVs. For further developments, we are planning to build additional testbed AUVs and adapt existing AUVs to our formation control demonstration system.

Acknowledgements

This work is supported by the Council for Science, Technology and Innovation (CSTI), Cross-ministerial Strategic Innovation Promotion Program (SIP), “Innovative Technology for Exploration of Deep Sea Resources” (Lead agency: Japan Agency for Marine-Earth Science and Technology, JAMSTEC). We gratefully acknowledge the assistance provided by Mr. Yuzuru Itoh (Ocean Engineering Research, Inc.), Mr. Kensuke Watari and Mr. Fumitaka Sugimoto (Offshore Technologies, LLC), as well as Mr. Tadashi Nimura and Mr. Katsuto Sakurai (Japan Offshore Design & Engineering Platform Technology & Engineering Research Association).

References

1) K. Kim and T. Ura: A Cruising AUV r2D4: Intelligent Multirole Platform for Deep-Sea Survey, J. Robot. Mechatron., Vol.26 No.2(2014), pp. 262-263.
2) Y. Nishida, T. Ura, T. Nakatani, T. Sakamaki, J. Kojima, Y. Itoh, and K. Kim: Autonomous Underwater Vehicle “Tuna-Sand” for Image Observation of the Seafloor at a Low Altitude, J. Robot. Mechatron., Vol.26 No.4(2014) pp.519-521.
3) Y. Nishida, K. Nagahashi, T. Sato, A. Bodenmann, B. Thornton, A. Asada, and T. Ura: Autonomous Underwater Vehicle “BOSS-A” for Acoustic and Visual Survey of Manganese Crusts, J. Robot. Mechatron., Vol.28 No.1(2016), pp.91-94.
4) T. Maki, Y. Noguchi, Y. Kuranaga, K. Masuda, T. Sakamaki, M. Humblet, and Y. Furushima: Low-Altitude and High-Speed Terrain Tracking Method for Lightweight AUVs, J. Robot. Mechatron., Vol.30 No.6(2018), pp.971-979.
5) A. Okamoto, T. Seta, M. Sasano, S. Inoue, and T. Ura: Visual and Autonomous Survey of Hydrothermal Vents Using a Hovering-Type AUV: Launching Hobalin Into the Western Offshore of Kumejima Island, Geochemistry, Geophysics, Geosystems, Vol.20 No.12(2019), pp.6234-6243.
6) Y. Nishida, T. Sonoda, S. Yasukawa, K. Nagano, M. Minami, K. Ishii, and T. Ura: Underwater Platform for Intelligent Robotics and its Application in Two Visual Tracking System, J. Robot. Mechatron., Vol.30 No.2(2018), pp.238-247.
7) T. Sato, K. Kim, S. Inaba, T. Matsuda, S. Takashima, A. Oono, D. Takahashi, K. Oota, and N. Takatsuki: Exploring Hydrothermal Deposits with Multiple Autonomous Underwater Vehicles, Proc. of the 2019 IEEE Underwater Technology (UT), Kaohsiung, Taiwan(2019), pp.1-5.
8) A. P. Aguiar and J. P. Hespanha: Trajectory-Tracking and Path-Following of Underactuated Autonomous Vehicles with Parametric Modeling Uncertainty, Proc. of the IEEE Trans. Automatic Control, Vol.52 No.8(2007), pp.1362-1379.

9) P. Millán, L. Orihuela, I. Jurado, and F. R. Rubio: Formation Control of Autonomous Underwater Vehicles Subject to Communication Delays, IEEE Trans. on Control Systems Technology, Vol.22 No.2(2014), pp.770-777.
10) B. Das, B. Subudhi, and B. B. Pati: Adaptive sliding mode formation control of multiple underwater robots, Archives of Control Sciences, Vol.24 No.4(2014), pp.515-543.
11) P. Ghorbanian, S. G. Nersesov, and H. Ashrafiuon: Obstacle avoidance in multi-vehicle coordinated motion via stabilization of time-varying sets, Proc. of the 2011 American Control Conf.(2011), pp.3381-3386.
12) X. Xiang, B. Jouvencel, and O. Parodi: Coordinated Formation Control of Multiple Autonomous Underwater Vehicles for Pipeline Inspection," Int. J. Advanced Robotic Systems, Vol.7 No.1(2010), pp.75-84.
13) S. Li, X. Wang, and L. Zhang: Finite-Time Output Feedback Tracking Control for Autonomous Underwater Vehicles, J. Oceanic Engineering, Vol.40 No.3(2015), pp. 727-751.
14) P. L. Kempker, A. C. M. Ran, and J. H. van Schuppen: A formation flying algorithm for autonomous underwater vehicles, Proc. of the 2011 50th IEEE Conf. on Decision and Control and European Control Conf.(2011), Orlando, FL, pp.1293-1298.
15) Z. Yan, D. Xu, T. Chen, W. Zhang, and Y. Liu: Leader-Follower Formation Control of UUVs with Model Uncertainties, Current Disturbances, and Unstable Communication, Sensors, Vol.18 No.2(2018), 662.
16) J. A. Neasham, G. Goodfellow, and R. Sharphouse,: Development of the "Seatrac" miniature acoustic modem and USBL positioning units for subsea robotics and diver applications, Proc. OCEANS 2015 – Genova(2015), pp.1-8,
17) T. Seta, A. Okamoto, S. Inaba, and M. Sasano: Development of a new operating system software for a hovering-type autonomous underwater vehicle HOBALIN, Proc. of the 2017 11th Asian Control Conf. (ASCC)(2017), Gold Coast, QLD, pp.37-42.
18) Robot Operating System. https://www.ros.org/ [Accessed February 26, 2020]
19) K. Tanizawa, M. Ueno, H. Taguchi, and T. Fujiwara: Actual Sea Model Basin in NMRI (National Maritime Research Institute), Marine Engineering, Vol.48 No.6(2013), pp. 776-781(in Japanese).
20) M. Tsujimoto, M. Kuroda, K. Shiraishi, Y. Ichinose, and N. Sogihara: Verification on the Resistance Test in Waves Using the Actual Sea Model Basin, J. Japan Society of Naval Architects and Ocean Engineers, Vol.16(2012) pp.33-39.

Appendix Kinetic Model of the Testbed AUV

In the tank test described in Section 3, the motion of the virtual leader AUV was computed based on the equations of motions [A1–A2)] as follows. Scalars were written without parentheses, vectors were written in parentheses ( ), and matrices were written in square brackets [ ]. However, parentheses ( ) were also used as a symbol to indicate calculation priority. Coordinate transformations were handled in Euler angles (123 system). A_b, for example $X_{u|u|\delta\delta}$, is a coefficient of a force A due to a parameter B. All parameters were obtained by experiments and design calculations.

$$[\boldsymbol{M}](\dot{\boldsymbol{V}}) + [\boldsymbol{\tau}][\boldsymbol{M}](\boldsymbol{V}) = (\boldsymbol{F_F}) + (\boldsymbol{F_G}) \tag{1}$$

$$(\boldsymbol{M}) = \begin{bmatrix} m + a_{11} & 0 & 0 & 0 & mz_G & 0 \\ 0 & m + a_{22} & 0 & -mz_G & 0 & mx_G + a_{26} \\ 0 & 0 & m + a_{33} & 0 & -mx_G + a_{35} & 0 \\ 0 & -mz_G & 0 & I_{xx} + a_{44} & 0 & I_{xz} \\ mz_G & 0 & -mx_G + a_{53} & 0 & I_{yy} + a_{55} & 0 \\ 0 & mx_G + a_{62} & 0 & I_{zx} & 0 & I_{zz} + a_{66} \end{bmatrix} \tag{2}$$

$$\frac{d}{dt}\begin{pmatrix} \Phi \\ \Theta \\ \Psi \end{pmatrix} = \begin{pmatrix} P + Q\sin\Phi\tan\Theta + R\cos\Phi\tan\Theta \\ Q\cos\Phi - R\sin\Phi \\ Q\sin\Phi\csc\Theta + R\cos\Phi\csc\Theta \end{pmatrix} \tag{3}$$

$$(\boldsymbol{V}) = \begin{pmatrix} U \\ V \\ W \\ P \\ Q \\ R \end{pmatrix} \tag{4}$$

$$\frac{d}{dt}(\boldsymbol{V}) = (\dot{\boldsymbol{V}}) = \begin{pmatrix} \dot{U} \\ \dot{V} \\ \dot{W} \\ \dot{P} \\ \dot{Q} \\ \dot{R} \end{pmatrix} \tag{5}$$

$$(\boldsymbol{F_F}) = \begin{pmatrix} X \\ Y \\ Z \\ L \\ M \\ N \end{pmatrix} \tag{6}$$

$$[\boldsymbol{\tau}] = \begin{bmatrix} 0 & -R & Q & 0 & 0 & 0 \\ R & 0 & -P & 0 & 0 & 0 \\ -Q & P & 0 & 0 & 0 & 0 \\ 0 & 0 & 0 & 0 & -R & Q \\ 0 & 0 & 0 & R & 0 & -P \\ 0 & 0 & 0 & -Q & P & 0 \end{bmatrix} \tag{7}$$

$$(\boldsymbol{F_F}) = (\boldsymbol{F_{HR0}}) + (\boldsymbol{F_{\Delta R}}) + (\boldsymbol{F_P}) \tag{8}$$

$$(\boldsymbol{F_{HR0}}) = -\begin{bmatrix} 0 & 0 & 0 & 0 & 0 & 0 \\ 0 & Y_v & 0 & 0 & 0 & Y_r \\ 0 & 0 & Z_w & 0 & Z_q & 0 \\ 0 & 0 & 0 & L_p & 0 & 0 \\ 0 & 0 & M_w & 0 & M_q & 0 \\ 0 & N_v & 0 & 0 & 0 & N_r \end{bmatrix} \begin{pmatrix} U \\ V \\ W \\ P \\ Q \\ R \end{pmatrix} - \begin{pmatrix} X_{u|u|} \\ 0 \\ 0 \\ 0 \\ 0 \end{pmatrix} U|U| \tag{9}$$

$$(\boldsymbol{F_{\Delta R}}) = \begin{bmatrix} 0 & 0 & 0 & 0 \\ Y_{u|u|\delta} & 0 & -Y_{u|u|\delta} & 0 \\ 0 & Z_{u|u|\delta} & 0 & -Z_{u|u|\delta} \\ L_{u|u|\delta} & L_{u|u|\delta} & L_{u|u|\delta} & L_{u|u|\delta} \\ 0 & M_{u|u|\delta} & 0 & -M_{u|u|\delta} \\ -N_{u|u|\delta} & 0 & N_{u|u|\delta} & 0 \end{bmatrix} \begin{pmatrix} \delta_1 \\ \delta_2 \\ \delta_3 \\ \delta_4 \end{pmatrix} U|U| - \begin{bmatrix} X_{u|u|\delta\delta} & X_{u|u|\delta\delta} & X_{u|u|\delta\delta} & X_{u|u|\delta\delta} \\ 0 & 0 & 0 & 0 \\ 0 & 0 & 0 & 0 \\ 0 & 0 & 0 & 0 \\ 0 & 0 & 0 & 0 \end{bmatrix} \begin{pmatrix} \delta_1^2 \\ \delta_2^2 \\ \delta_3^2 \\ \delta_4^2 \end{pmatrix} U|U| \tag{10}$$

$$(\boldsymbol{F_P}) = \begin{pmatrix} \eta_H\left(-X_{un|n|}U + X_{n|n|}\right)n|n| \\ 0 \\ 0 \\ -L_{n|n|}n|n| \\ 0 \\ 0 \end{pmatrix} \tag{11}$$

$$(\boldsymbol{F_G}) = \begin{pmatrix} -m_w g \sin\Theta \\ m_w g \sin\Phi \cos\Theta \\ m_w g \cos\Phi \cos\Theta \\ -m_{zR} \sin\Phi \cos\Theta \\ (-m_{xR} \cos\Phi \cos\Theta - m_{zR} \sin\Theta) \\ m_{xR} \sin\Phi \cos\Theta \end{pmatrix} \tag{12}$$

$$m_{xR} = mgx_G - \rho\nabla g x_B \tag{13}$$

$$m_{\boldsymbol{zR}} = mg\boldsymbol{z}_G - \rho\nabla g \boldsymbol{z}_B \tag{14}$$

$$m_w = \rho\nabla - m \tag{15}$$

where,

m	: mass
a_{ij}	: added mass or added moment of inertia
x_G, y_G, z_G	: center of gravity
x_B, y_B, z_B	: center of buoyancy
I_{ij}	: moment of inertia
U, V, W	: velocity (surge, sway, heave)
Φ, Θ, Ψ	: attitude angle (roll, pitch, yaw)
P, Q, R	: angular velocity (roll, pitch, yaw)
X, Y, Z	: fluid force excluding added mass
L, M, N	: fluid moment excluding added mass
$\boldsymbol{F_F}$	: fluid force excluding added inertia force
$\boldsymbol{F_G}$	: gravity and restoring force
n	: rotation speed of thruster
g	: gravity acceleration
ρ	: density of water
∇	: volume of displacement
$\delta_1, \delta_2, \delta_3, \delta_4$	: rudder angle (1: top, 2: starboard, 3: bottom, 4: port) *
$\boldsymbol{F_{HR0}}$	: resistance force vector of hull and rudder
$\boldsymbol{F_{\Delta R}}$	: rudder force vector with rudder angle
$\boldsymbol{F_P}$	: thruster force vector

* The rudder rotation coordinates are defined by a right-handed rotation system around a rudder axis that is positive on the AUV side and negative on the outside.

The equations were included stability, resistance, propeller, and wing theories [A3] in addition to the maneuverability theory. The equations were confirmed through comparing model test and numerical simulation results [A4].

To obtain the unknown coefficients, the following AUV motion tests were performed: resistance, oblique towing, PMM (surge, pure sway, and pure yaw), towing for measurement of rudder forces, free oscillation (roll and pitch), self-propulsion, circle, and zig-zag.

A1) B. H. Jun, J. Y. Park, F. Y. Lee, P. M. Lee, C. M. Lee, K. Kim, Y. K. Lim, and J. H. Oh: Development of the AUV 'ISiMI' and a free running test in an Ocean Engineering Basin, Journal of Ocean Engineering, Vol.36, Issue 1(2009), pp.2-14.

A2) T. Prestero: Verification of a Six-Degree of Freedom Simulation Model for the REMUS Autonomous Underwater Vehicle, the Joint Program in Applied Ocean Science and Engineering on 10 August 2001

A3) K. Kato, A. Oya, K. Karasawa: Introduction to aerodynamics, Publications of University of Tokyo, (1982), (in Japanese).
A4) S. C. Hirao, T. Fujiwara, A. Okamoto, H. Sekiguchi, M. Imasato, and M. Sasano: Study on Maneuvering Motion Modeling of Small AUV, J. the Japan Society of Naval Architects and Ocean Engineers, Vol.32(2020), pp.259-267.